Density profiling of polymers

K. T. Gillen, R. L. Clough and N. J. Dhooge
Sandia National Laboratories, Albuquerque, NM 87185, USA
(Received 26 April 1985)

This paper reviews the density profiling technique, a new, inexpensive and versatile analytical method which can yield extremely useful information on heterogeneities in polymers. The technique uses a density gradient column to monitor the density of a series of successive slices cut across a sample. A major application of the technique involves oxidation studies of polymers, since oxidation reactions usually lead to substantial increases in polymer density. Some representative examples of the utility of the technique are given, including the study of oxygen-diffusion-limited degradation, material incompatibility effects and chemical dose-rate effects in high-energy radiation environments.

(Keywords: oxidation; diffusion; density; profiling; diffusion-limited oxidation; ageing)

INTRODUCTION

Polymers that are exposed to air often have degradation processes dominated by oxidation. Important oxidation effects are observed in most ageing environments, which include elevated temperature, u.v. light, high-energy radiation and mechanical stress. Exposure of polymers to the air often leads to inhomogeneously oxidized samples, which complicates attempts both to understand the oxidation processes and to extrapolate accelerated exposures to long-term, real-time conditions. Inhomogeneous oxidation can result from either initially inhomogeneous material or from incompatibility problems with neighbouring materials.

Inhomogeneous oxidation can also be caused by oxygen-diffusion limited degradation. This well-known effect[1-3] occurs whenever the rate of oxygen consumption in the polymer is greater than the rate at which oxygen from the surrounding atmosphere can be resupplied to the interior by diffusion processes. The importance of this effect will therefore depend upon material geometry, the oxygen consumption rate and the oxygen permeation rate.

Attempts are often made to eliminate diffusion anomalies in ageing tests by studying thin samples. This approach has several potential problems. First the thin sample may not be thin enough, since oxidation depths may reach only fractions of a millimetre under typically-used, laboratory ageing conditions. Secondly, the properties of the specially-prepared thin sample may be unrepresentative of the bulk material, due either to different curing conditions or because ageing of these laboratory samples may overlook dominant degradation effects caused by the lack of impurities introduced during processing of the real materal. These impurities may be responsible for important degradation effects[4].

The authors have been interested in developing techniques for both monitoring heterogeneous oxidation and understanding the underlying mechanisms[4-6] for commercial as well as laboratory-prepared samples. The goal is to develop techniques capable of mapping inhomogeneous degradation across samples with thicknesses as small as 1 mm or less. A number of previous approaches have been used successfully for certain special types of materials. When ageing leads to measurable colour changes, colour development can be monitored[7]. For initially non-crosslinked materials, the depth dependence of crosslinking *versus* scission processes has been followed using solubility measurements[8] and gel permeation chromatography[7].

This paper describes in detail a new technique which is referred to by the authors as 'density profiling'. The technique depends on the observation that significant changes in density usually occur during oxidation of polymeric samples. Since the density of extremely small samples can be accurately monitored using a density gradient column, changes in density which occur over very small distances can be obtained. The technique can be applied to a large variety of materials, regardless of opacity or crosslinking. Representative data for samples aged in heat, u.v. radiation, high-energy (γ) radiation and under mechanical stress environments are given to show the utility of density profiling for recognizing the existence of heterogeneous oxidation, mapping the shapes of oxidation profiles and aiding in the elucidation of the oxidation mechanisms.

Two additional profiling methods, involving the optical examination of reflected light from cross-sections of metallographically polished samples and the profiling of relative hardness across these samples, have been described recently[5]. These techniques yield information complementary to density profiling.

EXPERIMENTAL

Materials

The six materials studied were commercial formulations. Three were cable insulation materials: a chemically crosslinked polyethylene (CLPE), a non-crosslinked low density polyethylene (PE) and an ethylene–propylene rubber (EPR). The other three materials were obtained in sheet form and included a polypropylene material and two materials used in seal and gasket applications (an ethylene–propylene rubber and a nitrile rubber).

0032-3861/86/020225-08$03.00

Ageing exposures

Heat ageing and high-energy γ-irradiations were carried out in Sandia's ageing facilities, which have been described in detail elsewhere[9]. During the ageing process, a steady flow of air was supplied to the sample chambers at a rate equivalent to approximately two changes of atmosphere every hour. Ultra-violet ageing was carried out in a Rayonet photochemical reactor.

Tensile measurements

Tensile tests were performed using a Model 1130 Instron with an electrical tape extensometer clamped to the sample. Samples were strained at 12.7 cm min^{-1} with an initial jaw separation of 5.1 cm. Elongation at break and ultimate tensile strength were measured at room temperature.

Sample preparation

The polypropylene material was aged in sheet form, whereas the nitrile rubber and EPR seal materials were cut from sheet material and aged as rectangular strips of approximate dimensions 0.6 cm × 15 cm. The remaining materials were cable insulations which had their copper conductors (either single or seven-stranded) removed prior to ageing. In this way air (oxygen) was available during the ageing both on the outside and inside (normal position of the conductor) of the insulation. The upper part of *Figure 1* shows sketches of a sheet sample and of cross-sections through one- or seven-conductor insulation samples and indicates how density samples are obtained. Sectors are cut for the insulation samples such that the overall density results will represent the average insulation density.

Various methods can then be used to obtain the thin slices (~50–250 μm) needed for density profiling and shown in the lower part of *Figure 1*. The crudest method involved slicing the sample with a hand-held razor blade. Although this method can be difficult if thin slices are required, it is usually satisfactory for thicker slices, for screening studies and for instances where semi-quantitative profiles are sufficient. In principle, microtoming techniques should yield uniform thin slices. In practice, especially for elastomeric materials, we had

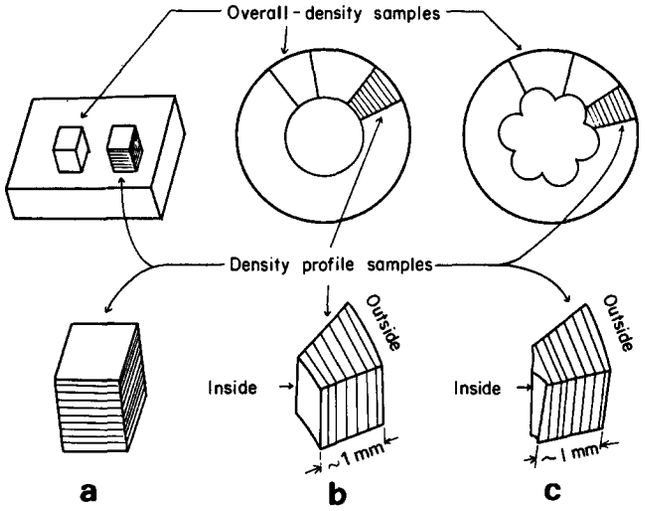

Figure 1 Schematic illustrating how overall density samples and density profile samples were obtained for three types of materials. a: sheet materials; b: single-conductor insulation samples; c: seven-conductor insulation samples

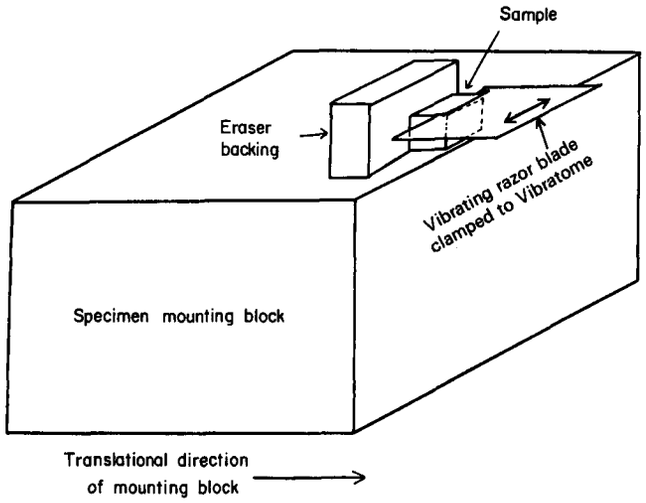

Figure 2 Schematic representation of the experimental arrangement used to obtain density profile samples using the Lancer Vibratome sectioning system

difficulty achieving satisfactory results with most standard one-pass microtomes. However, by using a Lancer Vibratome Series 1000 sectioning system, which involves a vibrating razor blade, it was possible to achieve reproducible results, even for elastomers. A schematic of the arrangement is shown in *Figure 2*. Overall-density samples are glued (using a cyanoacrylate adhesive) to the top and approximately flush with the leading edge of a mounting block. For horizontal support during the slicing, a piece of eraser larger than the sample is first glued behind and adjacent to the intended location of the sample, and the sample is then mounted flush against the eraser. The uniformity of the slices for a given material will depend on the size and stiffness of this backing material. For rubbery materials, it was found that a soft art gum eraser gives good results. By utilizing a Vibratome blade angle of 0° (blade parallel to slicing direction), half-length razor blades, maximum back and forth blade amplitude, minimum forward speed of the clamped mounting block and water lubrication, it was possible to obtain uniform slices down to thicknesses of ~25–50 μm for most elastomeric materials. The best results are achieved using the thin blades obtained by dismantling twin shaving blades available from numerous commercial manufacturers.

After slicing, a micrometer is used to assess the uniformity in thickness across each slice and to estimate its average thickness. For data presentation, we take the overall sample thickness to be the summation of the estimated average thicknesses of its slices. This allows us to calculate the relative positioning of each slice with respect to the material's cross-section. For a profile of a sheet material, the relative positioning of slices is defined quantitatively but the situation becomes less quantitative for more complicated cross-sections, such as near the inside surface of the insulation material removed from seven-stranded conductors.

Density column procedures

Normal procedure for creating a density column involves gravity-fed mixing of high and low density liquids. Since there were difficulties creating linear columns with predictable density ranges utilizing such techniques, a modified mixing procedure based on liquid

pumps was used. This is shown schematically in *Figure 3*. The flasks marked A and C contain respectively the high and low density liquids, which were mixed to create the gradient column. The pumps B and E are Cole Parmer Masterflex peristaltic pumps [model nos. 7543-06 and 7543-12 respectively], chosen so that the liquid pumping rate of pump E ($\approx 500\ cm^3\ h^{-1}$ using 3 mm inside diameter Tygon tubing) was twice that of pump B. The output of pump B was fed into flask C; efficient mixing is achieved using a magnetic stirrer D. It was found that this arrangement gave columns with good linearity and predictable density ranges.

Our gradient columns (available from SGA Scientific Inc.) are of concentric double wall construction, which allow temperature control with a circulating bath set at 23°C. The columns are calibrated using glass calibration balls of known density (measured at 23°C) which were obtained from Techne, Inc. Typical column resolution is 0.002 g cm^{-3} per cm of column height.

For measurements above 1.0 g cm^{-3}, columns were made using calcium nitrate–water solutions; below 1.0 g cm^{-3}, water–ethanol solutions were used. Many factors need to be considered when choosing the liquids for a column. Our primary criterion was avoiding selective absorption problems[10,11], where substantial density errors can result. For polyolefin materials, this problem is usually insignificant in columns containing water and ethanol due to their limited solubilities (typically less than 0.05% by volume). Most other candidate organic liquids, such as *p*-xylene, CCl_4, toluene and chlorobenzene, have much larger solubilities, and can therefore yield large selective absorption errors. Since changes in density caused by oxidation are of primary interest and oxidation can effect selectivity, there is another reason to avoid such columns. Another advantage of using columns made from ethanol and water is the lack of toxicity.

The possibility that surface effects could cause errors in ethanol–water columns has been addressed in two careful studies[10,11], both of which concluded that such effects are not significant. To confirm these conclusions, some of the ethanol–water density results were compared with

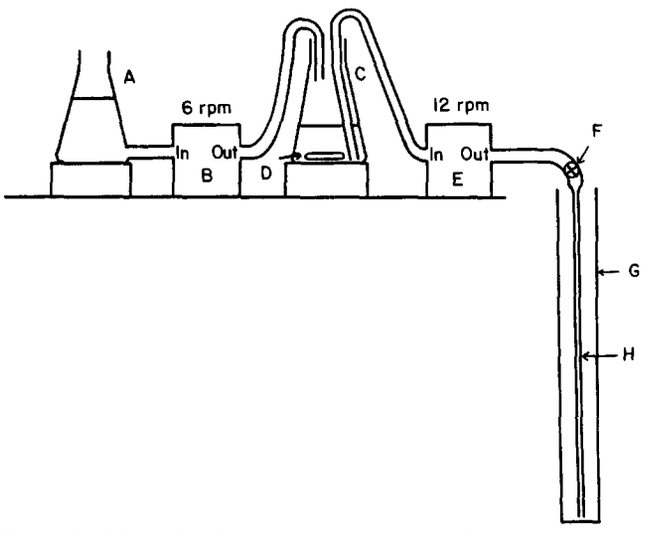

Figure 3 Schematic of the experimental set-up used to prepare density gradient columns. A and C are flasks that contain the high density and low density solutions respectively. B and E are liquid pumps chosen such that the pumping rate of E is approximately twice that of B. D is a magnetic stirrer used to ensure efficient mixing of the two solutions. H is a capillary tube used to fill the gradient tube, G

measurements taken in alternative organic mixtures. No significant differences were observed. For instance the density of the unaged polyethylene material was measured as 0.925 ± 0.002 g cm^{-3} in ethanol–water (after 15 min, with no change 3 days later) and 0.923 ± 0.002 g cm^{-3} in toluene–chlorobenzene (after 15 min). Because of the selective sorption of toluene, however, the latter result slowly dropped to 0.919 ± 0.002 g cm^{-3} after 3 days.

Since air bubbles attached to samples will result in density values which are lower than normal, proper wetting of samples prior to introduction into the column is another concern. Using a microscope, the surfaces of the samples can be examined for air bubbles after placement in the bottom of a shallow glass dish containing a solution of density lower than the sample. In instances where air bubbles are a problem, the sample can be wet after pumping on a vacuum system. A second approach, which was found to be useful for certain materials, involves improving their wettability by treating them for a few minutes with an argon plasma. Another possible approach, which has not been attempted, involves the use of surfactants.

Density measurements

After introduction to the top of a density gradient column, the sample falls until it reaches the point at which the liquid density in the column equals the sample density. The time to reach this position depends on the sample shape and size, and on the gradient fluid viscosity. Large samples ($\sim 1\ mm^3$) reach equilibrium in a few minutes, whereas small samples may require many hours.

Some simple observations and experiments can be used to eliminate any remaining problems over the possible presence of small air bubbles, not observed with the microscope, and artifacts caused by selective absorption of a column liquid. When the materials selectively absorb liquid of density lower than the sample (e.g. water from a salt–water column), the sample will first sink to a minimum in the column and then start floating upwards as the absorption continues to swell the material. It can be argued that during the long times required for small samples to reach equilibrium in the column, this sorption process may achieve equilibrium. Thus, a minimum followed by a rise in the column might not be observed even in the presence of significant swelling. Large samples, however, approach equilibrium density conditions within minutes, a time much smaller than it takes for sorption equilibrium, given the larger sample dimensions coupled with the smaller time. If selective sorption of the less dense liquid occurs for these samples, they will then slowly rise (or fall if higher density fluid selectively absorbs) over a much longer time scale[10]. In this way, problems involving selective sorption effects are eliminated in screening experiments where overall density samples (*Figure 1*) of varying size are observed in the column. If these screening tests show that the equilibrium density is independent of sample size, problems involving microscopic air bubbles are also eliminated, since the surface to volume ratio increases significantly as the sample size decreases. A second and similar check for possible artifacts such as small bubbles involves comparison of the overall sample-density with the weighted average density of the slices used for profiling the sample. It should also be mentioned that the importance of sorption can change as a material

becomes oxidized, implying that these effects may appear for aged materials even if they are minimal for unaged materials.

For the materials and ageing conditions described in this study sorption problems were found to be minimal. This result is expected for the polyolefin materials, since water and alcohol sorption is typically small. Water sorption effects for a plasticized PVC and for a chloroprene rubber were observed. This made interpretation of density data more difficult. For these materials, a column made from different liquids might be more useful.

RESULTS AND DISCUSSION

Representative results for radiation-aged materials

The ageing mechanisms underlying degradation of polymeric materials in high-energy radiation environments can be complex[4–6]. In the presence of air (oxygen), radiation dose-rate effects and synergy of radiation and temperature are often observed. These effects, which must be understood to make confident predictions about material responses, can be divided into two types: physical and chemical. Physical dose-rate effects are common during radiation exposures, and are caused by diffusion-limited oxidation. At high dose rates dissolved oxygen is used up faster than it can be replenished from the surrounding atmosphere. This results in more oxidation near air-exposed surfaces and less in the interior. As the dose-rate is lowered, the oxidation will proceed further into the sample, leading eventually to a homogeneously-oxidized material. Chemical dose-rate effects occur whenever some step in the kinetics underlying degradation occurd on a time scale comparable to the sample exposure time.

It will be shown that density profiling is very useful in helping to elucidate these mechanisms. This will be done by describing some results for crosslinked polyethylene (CLPE) and low density polyethylene. *Figure 4* shows mechanical property data for the CLPE material aged at 43°C in a cobalt-60 radiation ageing facility[9]. The ultimate tensile elongation, e, and the ultimate tensile strength, T, divided by their unaged values, e_0 and T_0, are plotted against the integrated radiation dose at the indicated dose rates. Exposures were carried out under conditions of slow air flow, except for

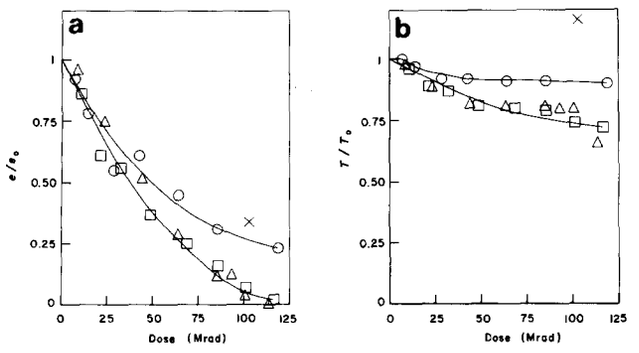

Figure 4 Mechanical property results for the radiation ageing of a chemically crosslinked polyethylene cable insulation material at 43°C. (a) The tensile strength after ageing divided by the tensile strength before ageing (T/T_0) and (b) the tensile elongation after ageing divided by the tensile elongation before ageing (e/e_0) are plotted *versus* the total integrated radiation dose under the various indicated dose rate and atmospheric conditions. (△): 17.5 krad h^{-1}, in air; (□): 64 krad h^{-1}, in air; (○): 890 krad h^{-1}, in air; (×): 1060 krad h^{-1}, in N_2

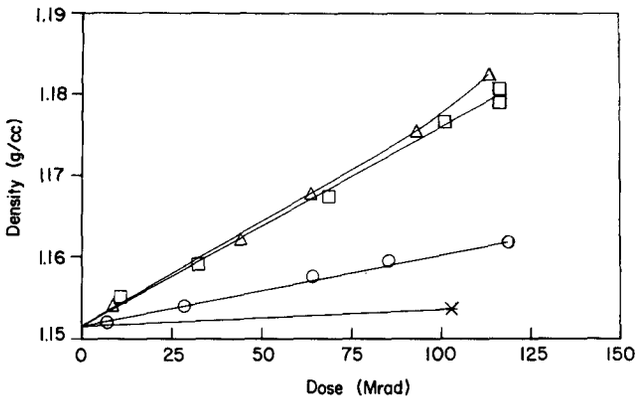

Figure 5 Overall density results for chemically crosslinked polyethylene cable insulation material. The density is plotted *versus* total radiation dose under the various indicated experimental conditions. (△): 17.5 krad h, in air; (□): 64 krad h, in air; (○): 890 krad h^{-1}, in air; (×): 1060 krad h^{-1}, in N_2

the points labelled with a cross, which refer to exposures in a nitrogen atmosphere. When the nitrogen and air ageing results are compared they clearly show that oxidation mechanisms are important for the degradation. In air environments, the mechanical deterioration appears to be sensitive to dose rate somewhere above 70 krad h^{-1}, but appears to be independent of dose rate below this level.

Overall density results for this material are shown in *Figure 5*. The slight increase in density for the sample aged in nitrogen should be noted. Many materials aged in nitrogen have similar small increases in density. Since weight increases are impossible in a nitrogen atmosphere, these results imply slight shrinkages in these materials, probably as a result of crosslinking caused by the radiation. However, the samples irradiated in air show large increases in density. In air environments, the sample weight will increase due to reactions which covalently bind oxygen, but decrease due to the formation of gaseous products such as H_2, CO_2, CO and CH_4. For radiation exposures at low to moderate temperatures in the presence of air, sample weights are usually found to increase, implying that the first mechanism dominates. Since this increase in weight is usually smaller than the density increase, overall shrinkage must occur in the material. The fact that the observed density increases are due to a combination of a weight increase coupled with a volume decrease is one major reason for the striking sensitivity of the overall density to the relatively subtle dose-rate effects noted for the mechanical properties.

In the air environments, the effect of dose rate on the overall density results for CLPE (*Figure 5*) show excellent correlation with the mechanical property results of *Figure 4*. It should also be noted that the overall density depends approximately linearly on dose. This linearity implies that the reactions responsible for the degradation are not time-dependent; in other words, the oxidation is not autocatalytic. Reaching a similar conclusion from data less directly related to the chemical reactions (e.g. mechanical property data) would be difficult.

Results from density profiling are even more instructive than those from overall density. *Figure 6* shows density profiles for unaged CLPE and samples radiation-aged in air to approximately 115 Mrad at the three indicated dose rates. A straight horizontal line was drawn for the unaged material, since the variation in density across unaged samples was found to be less than ± 0.001 g cm^{-3}. For

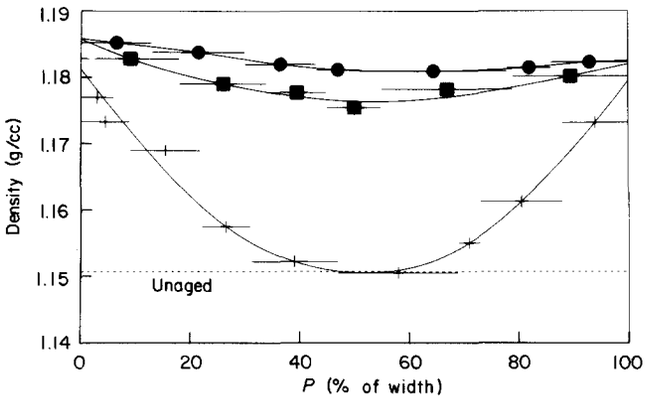

Figure 6 Density profiles for an unaged sample of chemically cross-linked polyethylene material and for three samples radiation-aged in air to approximately the same total dose – (●): 113.5 Mrad, at 17.5 krad h^{-1}; (■): 116 Mrad, at 64 krad h^{-1}; (+): 119 Mrad, at 890 krad h^{-1}. The percentage of the distance from the outside to the inside of the sample, *P*, is plotted as the abscissa. For this material, this distance averaged approximately 0.8 mm. (- - - -): unaged

aged samples, the density data for the series of slices taken across the sample were plotted as a series of horizontal bars. Each bar spans the region from which the slice was taken, measured as a percentage of the distance from the outside to the inside of the insulation. Under the high dose-rate ageing conditions, the oxidation is extremely heterogeneous with substantial oxidation near both the outside and inside surfaces (both of which were air-exposed) and essentially no oxidation in the middle of the sample. As the dose rate is lowered, the amount of heterogeneity decreases, with the result that at 17.5 krad h^{-1}, the oxidation of the sample is relatively constant across the cross section. These results offer unambiguous evidence that diffusion-limited oxidation is responsible for the dose-rate effects observed among the mechanical property data.

In addition to supplying useful information on physical diffusion processes, density profiles can be valuable for recognizing and understanding chemical dose-rate-effect processes. For instance, the CLPE profile data of *Figure 6* suggest that at the sample surfaces, the density increase due to oxidation is independent of dose rate. Since diffusion-limited effects are absent at the surfaces, this implies that chemical dose-rate effects are absent for this material over the range of the dose-rate conditions studied.

It is possible therefore to infer from the density results for this CLPE material that the oxidation rate is approximately time-independent, that chemical dose-rate effects are unimportant, and that physical diffusion effects become negligible below approximately 20 krad h^{-1}. This information is extremely valuable for predicting radiation ageing effects at low dose rates. Additional information on the kinetics underlying the oxidative degradation is available from detailed analyses of the profile shapes and their dependences on dose rate. These results will be discussed elsewhere[1,2].

Another example for radiation environments involves a case in which both physical and chemical dose-rate effects are significant. *Figure 7* shows normalized tensile elongation data for the low density polyethylene (PE) material plotted against total radiation dose. The material was aged in air at 43°C at the three indicated dose rates (3; 20; 946 krad h^{-1}). In contrast to the CLPE, the dose rate effects for this material are substantial, and give no indication of disappearing at low dose rates. Density profiles were obtained for badly degraded samples ($e/e \sim 0.1$) at each of the three dose rates and for an unaged sample. The unaged material had a flat profile with density equal to a constant value of 0.925 g cm^{-3}. As usual, the density of the oxidized materials increased with respect to the unaged density. For convenience of presentation, the observed changes in density for the aged samples were divided by the appropriate radiation dose (11, 23 and 114 Mrad respectively at 3, 20 and 946 krad h^{-1}). The resulting profiles in *Figure 8* therefore give the change in density per Mrad, plotted across the sample. These density profiles show that oxygen-diffusion limited degradation is very important at the highest dose rates, but becomes insignificant at the lowest.

Figure 9 shows the density at the outer edge of the polyethylene samples plotted *versus* dose at the three indicated dose rates (3; 20; 946 krad h^{-1}). For a constant total dose, the change in edge density increases by a factor of ~6 in going from 946 krad h^{-1} to 3 krad h^{-1}. Since the edge density is unaffected by diffusion effects, these results indicate that chemical dose-rate mechanisms are partly responsible for the mechanical property dose-rate effects. Easy recognition of the conditions under which the physical diffusion mechanism disappears, and ready determination of when such chemical effects exist, underscore two of the reasons for the utility of density profiling. For this PE material, a major

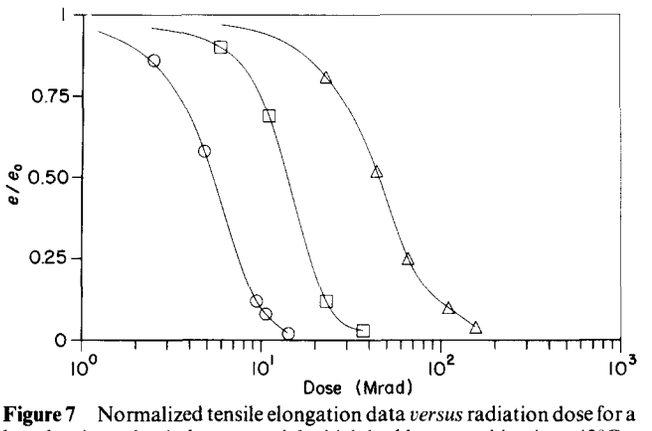

Figure 7 Normalized tensile elongation data *versus* radiation dose for a low density polyethylene material which had been aged in air at 43°C – (○): 3 krad h^{-1}; (□): 20 krad h^{-1}; (△): 946 krad h^{-1}

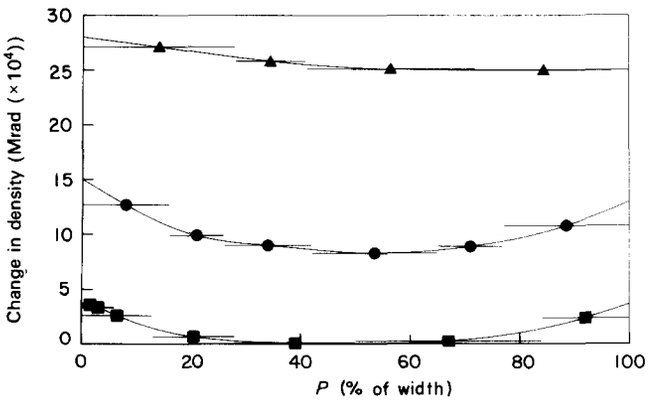

Figure 8 Profiles of the change in density per Mrad of radiation dose for three samples of the low density polyethylene material, which were aged in air – (▲): 3 krad h^{-1}; (●): 20 krad h^{-1}; (■): 946 krad h^{-1}. *P* represents the percentage of the distance from the outside edge to the inside edge of the sample. This distance averaged approximately 0.8 mm for this material

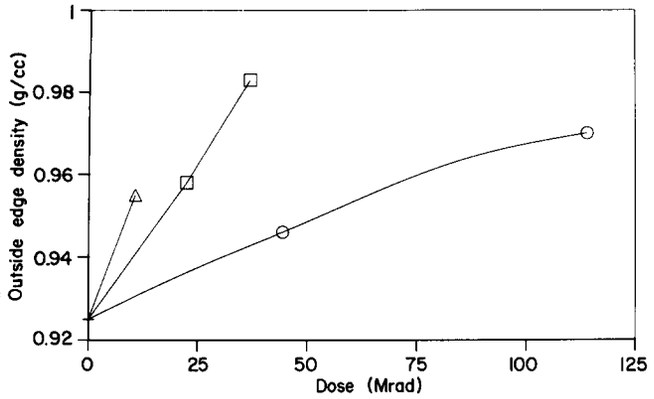

Figure 9 Density at the outer edge of the polyethylene insulation material plotted *versus* radiation dose – (△): 3 krad h^{-1}; (□): 20 krad h^{-1}; (○): 946 krad h^{-1}

contributor to the chemical mechanism is the slow breakdown of the intermediate hydroperoxide species[6,13].

Representative results for thermally-aged materials

Oven ageing in air is the most commonly used method of estimating the service lifetime of a material (or component). The samples are aged at various temperatures which are higher than the application temperature. Using material properties monitored at each temperature, an attempt is made to extrapolate the elevated temperature results to the service temperature. The Arrhenius equation, which is widely used for thermal extrapolation, predicts that a plot of the log of the time to reach a specified amount of degradation *versus* the inverse absolute temperature should be linear. The goal of accelerated ageing is to accelerate all the important ageing processes (chemical and physical) equally with respect to normal conditions used and determine the acceleration factor[14]. The Arrhenius approach can only be justified in such instances. Since one major problem for the Arrhenius approach in air environments is the possible existence of oxygen-diffusion limited degradation, it is important to determine the accelerated conditions under which such effects occur. Density profiling provides a method of accomplishing this goal.

In typical elevated temperature environments, the mechanisms leading to density increases are slightly different from those discussed earlier for moderate to low temperature radiation exposures. Normally, the weight of gaseous products released during oxidation will be larger than the weight of covalently bonded oxygen added to the material. Thus, both the sample weight and volume will decrease, and since the volume decrease is usually faster, the density will tend to increase. In filled polymers, these increases will be much larger since weight loss of polymer will lead to an increase in the weight fraction of the higher density filler material (e.g. clay).

Figure 10 shows the density profiles for air–oven aged nitrile rubber samples of thickness ≈ 1.5 mm. The results in *Figure 10a* show an unaged profile and profiles for 2 day and 7 day exposures at 150°C. These conditions represent moderate and severe mechanical degradation, with the ultimate tensile elongation dropping to $\approx 60\%$ and 5% of the initial value, respectively. The unaged profile is not quite flat, probably due to slight thermal gradients during compression-moulding of the slabs used in the study. The profiles for the aged materials indicate that important oxygen-diffusion effects exist for both ageing times at 150°C, with very little oxidation occurring near the centres of the samples. *Figure 10b* shows profiles taken for samples aged for 7 days and 28 days at 130°C. These also correspond to moderate and severe mechanical degradation respectively. Diffusion effects for the severely degraded sample are significant but appear to be reduced compared with the result for the sample after 7 days ageing at 150°C. This is as anticipated since diffusion activation energies are normally lower than the activation energies for thermal oxidation. In contrast, the results for the moderately degraded sample at 130°C appear to indicate that diffusion effects are less important at earlier times. These results are consistent with a degradation rate that increases with ageing time. In other words, at earlier times, diffusion processes are capable of supplying sufficient oxygen to the sample interior, whereas at later stages in the degradation, the rate of oxygen consumption increases (and/or the diffusion rate of oxygen decreases) until this is no longer true. This result is in accord with the frequently observed phenomenon that thermal-oxidative degradation of many organic materials exhibits an induction period. That is, the oxidation of a material starts slowly, but accelerates with time.

When oxygen-diffusion effects lead to heterogeneously degraded samples, comparisons of material degradation parameters (e.g. mechanical property data) obtained at different temperatures must be viewed with suspicion. If extrapolations of elevated temperature data are attempted, diffusion effects need to be eliminated. One way of accomplishing this is to lower the exposure temperatures until homogeneously aged samples are confirmed.

Even when the experimental conditions eliminate diffusion effects, density profiling will often give other useful information. An example involves EPR cable insulation material. Oven ageing results for this material, covering a temperature range of 100°C–170°C, gave non-Arrhenius behaviour at both high and low temperatures. At the higher temperatures, some contribution from diffusion effects might be expected. However, given the relatively high oxygen permeation rate for EPR materials[15] coupled with the very long ageing times, diffusion effects under the lower temperature ageing conditions were not anticipated. This was confirmed by density profiling, but a second heterogeneous effect was observed. *Figure 11* shows density profiles for samples aged at the lowest ageing temperature and for an unaged sample. Very little change occurs with ageing except near the inside surface of the insulation, where dramatic density

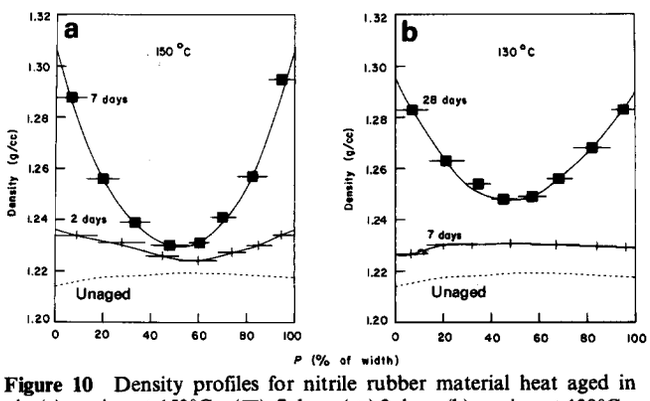

Figure 10 Density profiles for nitrile rubber material heat aged in air. (a): ageing at 150°C – (■): 7 days; (+) 2 days. (b): ageing at 130°C – (■): 28 days; (+) 7 days. (-----) unaged

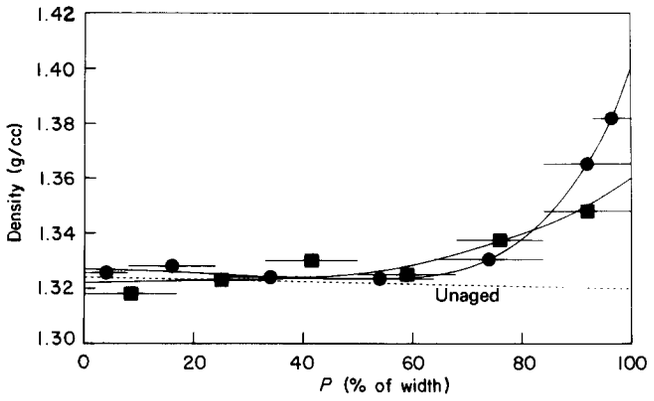

Figure 11 Density profiles for EPR cable insulation material which had been heat aged in air at 100°C – (■): 2062 h; (●): 7390 h

increases are noted. This enhanced oxidation near the inside of the insulation is due to catalysis by copper species, a mechanism which has been observed in numerous thermal oxidative studies of polyolefin materials[16–18] and also identifed using density profiling in room-temperature radiation exposures[4]. Although the EPR insulation samples were stripped from the copper conductors before ageing, copper salts could easily have diffused into the insulation during the high-temperature extrusion manufacturing process. Enhanced copper concentrations near the inside surface of the insulation were confirmed using emission spectroscopy and microprobe analysis.

Density profiling results at other temperatures indicate that the copper-catalysed oxidation mechanism has a higher activation energy than the normal oxidation of this material. This implies that as the temperature is lowered, the former becomes less important[12]. This explains the observed upward curvature of the Arrhenius curve. The observation that copper-catalysed oxidation can contribute significantly to the thermal degradation of this EPR material underscores the potential dangers inherent in material degradation studies that overlook possible material interactions. For instance, if thermal ageing studies were carried out on compression-moulded sheets of this material, copper-catalysed oxidation would not be observed.

Another useful aspect to the density profiling technique is that is is often very sensitive to the early stages of degradation. *Figure 12* shows mechanical property data versus time for this EPR material at 100°C. Comparing these data to the density profile data of *Figure 11* shows that significant changes occur in the density profiles before noticeable changes are apparent in the mechanical properties.

Other applications

A number of other applications of density profiling techniques to oxidation studies are apparent. For instance, materials aged in an ultra-violet environment may be heterogeneously oxidized due to oxygen-diffusion limited effects and/or attenuation of the u.v. radiation by the material. Density profiling results for a polypropylene material aged for 6 days in a Rayonet photochemical reactor are shown in *Figure 13*. Clearly, density profiling is capable of studying such effects.

Stress-relaxation studies are often used to predict material response for materials which are mechanically stressed, such as seals and gaskets. Again, reliable conclusions can be critically dependent upon eliminating diffusion effects from the accelerated simulations[19]. Density profiling offers a rapid and easy method for determining when such effects are present. *Figure 14* shows for example a density profile for ethylene–propylene seal material which was aged at a tensile strain of 15% for 69 h at 48°C and 850 krad h^{-1}. Even though the oxygen permeation rate in EPR materials is relatively

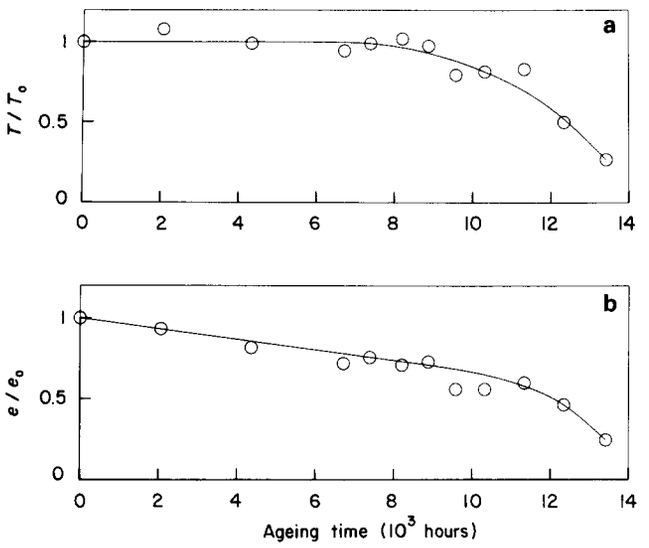

Figure 12 Mechanical property heat ageing results plotted *versus* time, at 100°C for EPR cable insulation material. (a) The tensile strength after ageing divided by the tensile strength before ageing (T/T_0) and (b) the tensile elongation after ageing divided by the tensile elongation before ageing (e/e_0)

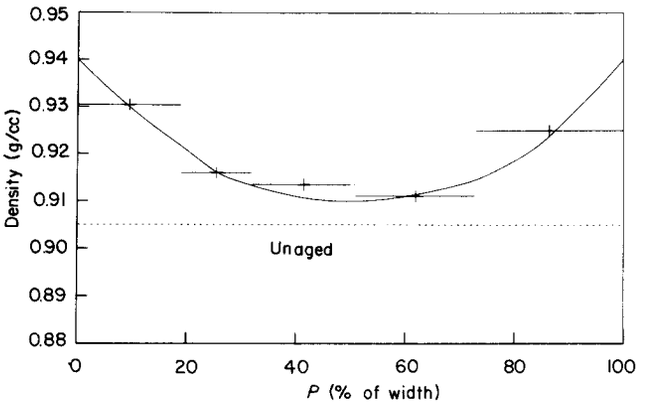

Figure 13 Density profiles of (- - - - -): unaged and (+): 3 day u.v. aged polypropylene samples

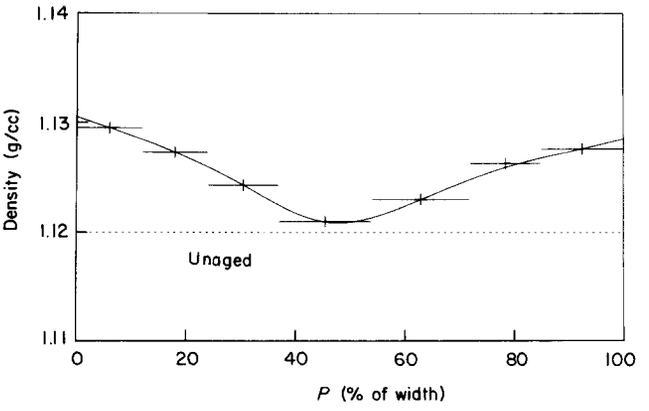

Figure 14 Density profile of an EPR O-ring material after exposure to mechanical tensile stress during radiation ageing: (+) and unaged: (-----)

high[15], significant diffusion effects occur under the above experimental conditions.

Another possible application is in studies of the diffusion of a material into a polymer. If the mixing leads to a density change which is larger than the variations in material density and the interdiffusion extends over at least 100–200 μm, density profiling may allow diffusion constants to be estimated.

CONCLUSIONS

Density profiling is an extremely sensitive, rapid and inexpensive analytical technique for studying polymers. Although it can be applied to unaged materials for determining whether material inhomogeneities exist and thus serve as a means of screening for insufficient component mixing or the possible presence of temperature gradients during cure, its main applications stem from the observation that large density increases can occur in air-ageing environments. Since the technique is capable of measuring the density of very thin (less than 25 μm) samples, it is ideal for investigating inhomogeneous oxidation mechanisms, such as diffusion-limited oxidation. This mechanism plays an important role in the degradation of numerous materials and can be induced by heat, high-energy radiation, u.v. light and mechanical stress. For ageing tests involving these environments either singly or in combination, the elimination of diffusion effects is critical to reliable predictions of material response under long-term exposures.

As well as providing an easy method for determining experimental conditions under which diffusion effects are no longer significant, density profiling is also useful for the determination and understanding of the chemical mechanisms important to oxidation. For instance, density profiling can yield information on whether oxidation reactions are constant with time or have autocatalytic behaviour. It is also useful for observing inhomogeneous oxidation effects near material interfaces caused by localized material poisoning or incompatibilities. In high-energy radiation environments, density profiling allows conclusions to be made about the existence of chemical dose-rate effects. We anticipate that many other applications of these techniques will be found. Two examples that come to mind are determining the attentuation of u.v. in a material through the use of oxidative depth profiles and estimating diffusion constants for the interpenetration of two materials.

ACKNOWLEDGEMENT

This work was supported by the US Nuclear Regulatory Commission as part of the Qualification Testing Evaluation Program conducted by Sandia National Laboratories under contract DOE 40-550-70, NRC FIN No. A-1051.

REFERENCES

1 van Amerongen, G. J. *Rubber Chem. Tech.* 1964, **37**, 1065
2 Matsuo, H. and Dole, M. J. *Phys. Chem.* 1959, **63**, 837
3 Cunliffe, A. V. and Davis, A. *Polym. Degr. Stab.* 1982, **4**, 17
4 Gillen, K. T. and Clough, R. L. *Radiat. Phys. Chem.* 1983, **22**, 537
5 Clough, R. L., Gillen, K. T. and Quintana, C. A. *J. Polym. Sci., Polym. Chem.* 1985, **23**, 359
6 Gillen, K. T. and Clough, R. L. *J. Polym. Sci., Polym. Chem.*, 1985, **23**, 2683
7 Bowmer, T. N., Cowen, L. K., O'Donnel, J. H. and Winzor, D. J. *J. Appl. Polym. Sci.* 1979, **24**, 425
8 Kuriyama, I., Hayakawa, N., Nakase, Y., Ogura, J., Yaguy, H. and Kasai, K. *IEEE Trans. El. Ins.* 1979, **EI-14**, 272
9 Gillen, K. T., Clough, R. L. and Jones, L. H. in 'Investigation of Cable Deterioration in the Containment Building of the Savannah River Nuclear Reactor', Sandia National Laboratories Report, SAND 81–2613 (August 1982)
10 Blackadder, D. A. and Keniry, J. S. *Makromol. Chem.* 1971, **141**, 211
11 Sharma, R. K. and Mandelkern, L. *Macromol.* 1969, **2**, 266
12 Gillen, K. T., unpublished results
13 Clough, R. L. and Gillen, K. T. *J. Polym. Sci., Polym. Chem.* 1981, **19**, 2041
14 Gillen, K. T. and Mead, K. E. in 'Predicting Life Expectancy and Simulating Age of Complex Equipment Using Accelerated Aging Techniques', Sandia National Laboratories Report, SAND 79–1561 (January 1980)
15 Seguchi, T., Hashimoto, S., Arakawa, K., Hayakawa, N., Kawakami, W. and Kuriyama, I. *Radiat. Phys. Chem.* 1971, **17**, 195
16 Chan, M. G. and Allara, D. L. *J. Colloid Interface Sci.* 1974, **47**, 697
17 Chan, M. G. and Allara, D. A. *Polym. Eng. Sci.* 1974, **4**, 12
18 Reich, L. and Stivala, S. 'Elements of Polymer Degradation', McGraw-Hill, New York, 1971
19 Ono, K., Kaeriyama, A. and Murakami, K. *J. Polym. Sci., Polym. Chem.* 1975, **13**, 2615